ORIGINAL RESEARCH ARTICLE

Evaluation of Modified Ti-6Al-4V Implant Surface Through β-Tricalcium Phosphate by Using Additive Mixed Electrical Discharge Machining for Biomedical Application

Behzad Oghazi, Hamid Baseri ⓘ, and Mahmoud Rabiee

Ti-6Al-4V alloy due to high mechanical properties and high corrosion resistance is widely used in the manufacture of biomedical devices, including hip articulations, screws and dental implants. For proper implant performance in the long run, a rapid reaction between the bone and implant should be performed, which depends on the surface properties of the layer doped on the surface of the implant. The surface coating is therefore considered to be the underlying factor in the attenuation of such occurrences. This research aims to assess the modified surface of Ti-6Al-4V by the mixed electric discharge (EDM) process of β-tricalcium phosphate powder to detect potential bioimplants. One of the features of this coating process is the location of the base titanium layer containing β-tricalcium phosphate, thereby improving the substrate properties. For investigating the surface morphology, distribution and dispersion of elements on the modified surface, field emission scanning electron microscope (FE-SEM), energy-dispersive x-ray spectroscopy (EDS) and x-ray diffraction (XRD) tests were used. Morphological features have shown that porous surface topography just like natural bone is coated on the surface of Ti-6Al-4V alloy using the AM-EDM process. EDS and XRD examinations showed the coated layer compositions from Ti kα, V, Al, Ca and P and also formation of the biocompatible phases such as $Ca_2P_2O_7$ and $Ca(OH)_2$ on the surface of Ti-6Al-4V, which caused the better biocompatibility of the alloy, creation of an antibacterial agent for periodical injuries and also improvement of the bone formation on the alloy surface. The results also showed that the size of the resin thickness was 35 micrometers, which contained nanoparticles of tricalcium phosphate, as well as an excellent metallurgical substrate with a strong bond between the substrate and the coating. In this research, the effects of input parameters, such as spark energy and powder concentration on output parameters, including material removal rate, surface roughness and surface hardness, were studied. The results showed that this method has a positive effect on the reduction in the material removal rate, roughness and hardness of the surface of the workpiece. Due to the dispersion of β-tricalcium phosphate particles, the surface roughness diminishes during the electric discharge process. Also, the highest material removal rate occurred in 21 A, the pulse duration of 50 μs and the concentration of 8 g/L, and minimal surface roughness occurred in 6 A, the pulse duration of 100 μs and the concentration of 4 g/L. The hardness of the surface deposited with β-tricalcium phosphate powder is 348 VH, which is 1.75 times more than the original surface. The reason is that the hard oxide is deposited on the surface of the workpiece.

1. Introduction

Titanium and its alloys are used to provide implants and tools used in clinical applications such as plates, screws and pins, which always come under repeated load conditions and fail to fatigue and corrosion. Biomedical implants, when exposed to the pervasive environment of the body, present deficiencies and holes in corrosion. Fleck and Eifler reviewed the fatigue performance of airborne titanium alloys and Ringer's solution. The fatigue efficiency of the buzzer solution is lower than that of air. The fatigue performances of the Ti-TiO 6Al-7Nb (α + β) and Ti-6Al-4V types are significantly superior to those of the CP-Ti alloy (Ref 1). The function of fatigue depends on the microstructure of titanium alloys, the manufacturing process and the heat recovery method (Ref 2-4). Williams and Chowola recently reported that in the neck region of the hip implant Ti-6Al-4V alloys show abrasion and corrosion cracking due to reduced fatigue resistance (Ref 5). The electrical discharge machining (EDM) method is based on the principle of material removal by local melting followed by evaporation using sparks formed in the insulating dielectric liquid without applying any mechanical force. Many parameters such as the type of dielectric liquid, electrode, part materials, pulse current and pulse time determine the properties

Behzad Oghazi, Hamid Baseri, and Mahmoud Rabiee, Babol Noshirvani University of Technology, Babol, Iran. Contact e-mail: h.baseri@nit.ac.ir.

of the modified surface (Ref 6, 7). The growth of fatigue cracks occurs by the acid liquid in the body, resulting in an improvement of the corrosion crack that results from the failure of the joint. The reason for the early breaking of the implant is due to several reasons such as imperfect mechanical properties of the implant, the development of unintended tissue integrity between the living and artificial bones, and the weak surface of the implant, as well as the weak resistance to corrosion and wear of the implant. An alternative method of implant surface modification is offered. Enhancing the surface of a key change process is the density properties of materials by removing or adding materials to the implant surface (Ref 8). In other words, the improvement of the surface required to repair the bones. Previous research has shown that surface properties play an essential role in the formation of new bones as well as in tissue growth (Ref 9, 10). Surface properties such as surface roughness (Ref 11), surface topography (Ref 12), surface porosity (Ref 13), surface chemistry (Ref 14) and surface energy (Ref 15, 16) have a significant effect on the formation of new tissue and protein and collagen absorption during in vivo and in vitro studies (Ref 17, 18). Some of the different methods to improve the implant function surface include physical vapor deposition, chemical vapor deposition, laser ionization and coating. The use of these methods as a surface treatment for titanium alloys in the long term was not satisfactory due to weak adhesion, low strength in physical bonding and inability to bear load in a corrosive environment. Recently, the importance of using the electric discharge machining process (EDM) has been widely recognized in the construction of a biocompatible surface with a nanostructure that has a favorable effect on the biological dependence of human osteoblasts (Ref 19). In the process (EDM), the materials of the electrode tools and additives are transferred to the dielectric fluid on the surface of the workpiece. Material transfer through AM-EDM is thought to change the chemical content, mechanical properties and metallurgical surface of the machined surface. As a result, different layers are created on the surface of the workpiece. The characteristics of these layers are mainly related to electrode type, powder particles, dielectric fluid and machining parameter settings (Ref 20). Due to the acidity of the body fluid and the immune system's response to the foreign body, a solid and porous surface of the implant should be created to prolong the implant's long-term life span and to establish a strong bond between the bone and implant surfaces. The increase in surface hardness is reflected in corrosion and abrasion resistance between implants and bones (Ref 21). Surface roughness control: Due to the wear and tear caused by the production of spark in the process of electrical evaporation machining, the surface of the oxide, which contains a rich base of base alloy, oxygen and carbon, is produced. Studies have shown that roughness of the surface causes bone tissue formation, and for the stabilization of the bone with improved surface roughness, Ra = 7.8 μm is required (Ref 22). For long-term grafting, the biocompatibility and bioavailability of implants are key aspects of medicine. A strong mechanical link between implants and bone tissue regarding biological physics and the biological chemistry response called biologically active. The different biomedical materials of the interface differ in terms of adhesion, resistance and adhesion thickness (Ref 21). Biologically active glass, ceramic and calcium phosphate are the most widely used biochemical and biological agents. A good environmental layer that has bone-like structure and mechanical properties that cause tissue to grow and adhere

should be produced. Biocompatibility and biological activity of the implant depend not only on the properties of the material, but also on the implant production and the coating technique that the implant tolerates depends. AM-EDM is a novel sedimentation method that can be used to place a biocompatible and biological layer on the implant surface. The fixed oxide surface has a high hardness and reasonable biocompatibility and has medical applications, particularly in orthopedics and dentistry. The purpose of the present study is to use the AM-EDM process for deposition of β-tricalcium phosphate powder on Ti-6Al-4V alloy for orthopedic and dental applications. The mechanical properties and biocompatibility, the coated materials on the surface of the implant and the results of the non-power tests will be compared. Input parameter variables in these experiments include spark energy (as a function of pulse current and pulse on time), different concentrations of β-tricalcium phosphate powder and production parameter variables including material removal rate, surface roughness, surface porosity, surface hardness and compounds. The elements and phases formed on the surface are improved.

Chow and colleagues investigated the effect of adding silicone powder to water as a dielectric fluid in the microslit machining process at EDM. They used water for dielectricity to prevent environmental problems. They concluded that adding powder would increase the space between the tool and the piece. Water and powder can disperse electrical discharges, thereby improving both surface roughness and loading rates (Ref 23).

Xie and his collaborators studied the improvement of the surface of carbon-45 using electrodes produced by powder metallurgy and the addition of graphite powder in the dielectric oil of the EDM process. The results showed that at the modified surface, the TiC-rich layer was formed which has a high surface hardness of 1360-14920 HV and excellent corrosion resistance properties, which ultimately prevents mechanical corrosion and oxidation. They also stated that by increasing the amount of powder in the dielectric fluid, electrical discharges were randomly generated, ultimately reducing surface cracks (Ref 24).

Prakash et al. studied the effect of the EDM process with increasing powder on the titanium alloy of the beta phase (Ti-35Nb-7Ta-5Zr). They stated that a discontinuous reduction in surface cracks at a concentration of 4 g/lit may be observed by machining silicon powder. Also, in improving the Ti-β alloy at a current rate of 15A and a long pulse duration at a concentration of 8 gr/lit of powdered Si particles, a uniform surface porosity with openings of 200-500 nm was observed. At a concentration of 2 gr/lit of powder Si at 4 gr/lit, the amount of a recast layer from 8 micrometers to 2 to 3 micrometers, respectively. Elemental analysis in the PMEDM process shows that due to chemical reactions, the process is formed at the alloy, carbide and oxide surface, which results in increased biocompatibility as well as improved machining performance in increasing the material removal rate (MRR) and reduces the tool wear rate (TWR) (Ref 25).

Sahu et al. (Ref 26) examined Inconel 718 superalloys under SiC mixed EDM which resulted in a lower crack density of the machined surface, better surface morphology due to reduced surface irregularities and significant grain refinement. However, the powder concentration was not evaluated in the study and the researcher suggested an urgent need for the study based on different powder concentrations on the surface roughness (Ref 26).

Ndaliman and colleagues investigated the effect of two dielectric fluids on the increase in the superficial properties of the Ti-6Al-4V alloy by the EDM process. Urea and distilled water were treated as a dielectric fluid and Cu-TaC alloy as the electrode. The results show that when distilled water is used as a dielectric fluid, the roughness is higher than that of the urea solution, which is $R\,a_d = 14.45\,\mu m$ and $R\,a_o = 19.05\,\mu m$, respectively. They argued that machining with a urea solution would increase the surface hardness of the machine with a distilled water solution (Ref 27).

The literature has exposed that powder. Mixed EDM has a wider reach in changing the surface of different materials compared to other machining process (Ref 28). Ti-6Al-4V ELI (grade 23) is an alloy specifically designed for biomedicine implants requiring surface modification to enhance biocompatibility in vitro and vivo environments. The strength of the work was in deepening the surface characteristics produced by the process (EDM) which is used simultaneously for processing and surface modification. Furthermore, powder mixed EDM modification of the surface of Ti-6Al-4V ELI (grade 23) is explored to assess the impact of powder concentration, pulsation, current as well as a pulse on rest time on surface integrity for specialized applications in the biomedical field/ industry. In addition, the work focuses on improving the quality of the surface of the said material for the improvement of mechanical behavior and bioactivity (Ref 28).

Öpöz et al. (Ref 29) assessed surface roughness, deposited particles and surface topography. Ti-6Al-4V microhardness in SiC composite EDM. The study evaluated the pulse current, the pulse in the timeframes and concentration of powder using the electrode aluminum 6081 T6. The study shows only the concentration in powder was the most influential factor in the responses and RLT decreased by increasing the powder level, whereas the hardness of the layer increased as a result of material migration (Ref 29).

Alavi and Jahan (Ref 30) studied the effect of electrode coating (uncoated tungsten carbide, TN-coated tungsten carbide), servo voltage, capacitance and rotational speed on MRR, TWR, microhardness and crater size on Ti-6Al-4V. The study revealed that stress was an important factor for integration time and crater machining while capability was found to be significant on microhardness and TWR (Ref 30).

Mughaln et al. (Ref 31) investigation surface change for osseointegration of Ti-6Al-4V ELI using PMEDM. Pulsed current, on/off time and various levels of silicon carbide powder (SiC) are used as input parameters to understand the desired surface changes. The results showed powder concentration is considered as the most important factor to control surface roughness and recast layer depth and also oxides and carbides enriched surface improved the microhardness of the re-solidified layer from 320HV to 727HV (Ref 31).

Andreas et al. (Ref 32) were involved in the development in the confliction mechanisms and the effects of powder mixed EDM main machining conditions such as powder and electrical parameters on improving mechanical and antibacterial propertied as well as biocompatibility of the surface have been discussed. It has been shown that the material transfer of the powder suspension in the dielectric fluid significantly changed the functionalization of the surface. Depending on the selected powder material and material composition of the modified layer, the surface properties such as microhardness, corrosion resistance wear resistance, fatigue performance, biocompatibility and antibacterial have been significantly improved (Ref 32).

2. Materials and Method

2.1 Workpiece and Tools

The workpiece used for the tests is a titanium rod (Grad V) in size Ø6 × 40 mm (Ti-6Al-4V). This grade of alloys is a lightweight component.

For the tests, the electrode in pure titanium of size Ø12 × 35 mm was used. The surface of the workpiece and tool electrodes is sized with a forearm by turning machining, and before coating process using silicon carbide emery papers of grade 1000 and eventually cleans up by acetone solution.

2.2 Synthesized Powder

According to the research conducted in the field of coating by EDM process in this study, β-tricalcium phosphate $(\beta - TCP; Ca_3(PO_4)_2)$ powder was used to sedimentation the workpiece surface. The β-TCP was prepared by heating a mixture of 2 moles of Monetite and 1 mole of calcium carbonate in the electric furnace. The product was crushed into the crusher to decrease particle size. Median β-TCP particle sizes determined by laser particle size and powder size analysis were prepared in granulation from 1 to 5 μm (Ref 33) and (Ref 34).

2.3 Dielectric and Tank

Deionized water was used as a dielectric in this project; to perform the coating process, a two-liter reservoir was used. The Tehran Ekram electrical discharge machining 304A (TE EDM 304A) was used to perform the coating tests. The detailed experimental characterization for the AM-EDM process is shown in Table 1. In addition, Fig. 1(a) shows a schematic of the electric discharge process with an additive mixed with β-TCP powder used in this study and Fig. 1(b) shows the actual photograph of EDM and separate experimental setup of additive mixed EDM technique.

2.4 Constant and Variable Parameters

In EDM process, the discharge energy are defined as:

$$E_d = \int_0^{t_d} u(t).i(t)\mathrm{d}t \cong U_\mathrm{d}I_\mathrm{d}t_\mathrm{d} \qquad \text{(Eq 1)}$$

Table 1 Parameters of experiments

| Name of parameter	Range of parameter
Polarity of tools	Positive
Polarity of workpiece	Negative
Generator type	Iso-Pulse
Dielectric type and dielectric volume	deionized water and 2 Liter
Powder type	β-tricalcium phosphate
Powder concentration	0, 4, 8, 12 (gr/lit)
Source voltage	250 (V)
Pulse-on time	35,50,100 (μs)
Pulse-off time	8 (μs)
Machining time	15 (min)
Surfactant-SDS	2 (gr)
Calcium chloride	0.1 (mol/lit)
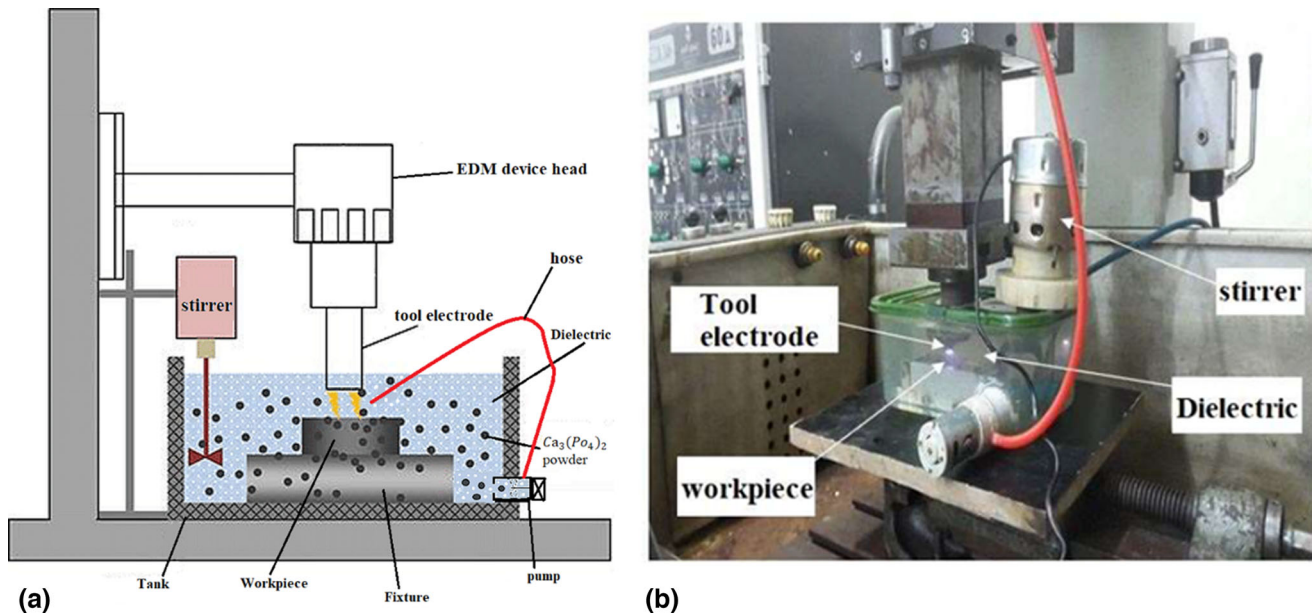
Fig. 1 (a) General scheme of the process (AM-EDM) 1. (b) Experimental setup of β-TCP mixed EDM process

where the discharge voltage, current and time are indicated by U_d, I_d and t_d, respectively; and $u(t)$ and $i(t)$ are the instantaneous voltage and current. From equation (1), it can be indicated that higher spark energy is generated by an increase in either U_d, I_d or t_d, which influences the surface modification. In our EDM, it can be selected only two values of 60 V or 250 V for U_d. The preliminary experiments showed that with the voltage of U_d = 250 V the roughness of the surface increases and the deposition of powder on the surface of the alloy is done to a more extent. Therefore, in this paper 2 parameters of I_d and t_d have been considered as variable parameters and the third parameter of U_d was selected as constant value 250 V.

Increasing the T_{on} causes more the energy and number of sparks, which eventually increases the light duration of the pulse. By adding powder, bridging phenomenon occurs, and with the increase Ton, the gap between two electrodes increases and causes a disruption in the performance of the process, and the surface of the alloy is less damaged. This phenomenon causes a decrease in resistance to the gap and ultimately leads to a better washing of the pollution and the displacement of the powders instead of the plasma channel.

$$R_g = \frac{\rho L}{A} \qquad (Eq\ 2)$$

In this relationship, R_g is the gap resistance, ρ is the fluid density, A is the cross-sectional area between the tool and the workpiece, and L is the length of the gap between the tool and the workpiece.

As T_{off} increases, the rinsing of the molten material improves considerably due to the increased time interval between two consecutive electric shocks, thereby improving the surface quality (Ref 35). However, MRR decreases because of the low spark intensity at high Toff. Conversely, smaller Toff values tend to increase the intensity of the spark which melts and vaporizes a larger amount of material in the machining area, thus increasing the MRR (Ref 35). However, there is a critical T_{off} value characterized by inadequate rinsing of the melted material. This causes the formation of craters and

microdefects on the machined surface, thereby increasing the roughness of the Ra surface (Ref 36).

In this study, for every experiment, an optimum machining time (15 minutes) is needed to form a stable plasma channel. Less than this time, the coating is done incompletely and more than this time will cause material removal rate form the surface and the formation of large pores and the roughness of the surface will increase.

Duty cycle is the ratio between the on time and the total pulse time that is represented as the following equation:

$$D = \frac{T_{on}}{T_{on} + T_{off}} \times 100 \qquad (Eq\ 3)$$

In high D, the applied spark energy results in a higher processing efficiency. Therefore, for applying the different duty cycle, the constant parameter of T_{off} = 8 μs and different values of T_{on} = 35, 50 and 100 μs were selected for achieving the duty cycles of 81.4, 86.2 and 92.6%, respectively. Tables 1 and 2 show the process parameters.

2.5 Method of Testing

Furthermore, to determine the effect of the powder concentration on the output parameters in a separate experiment, 12 g/ml of powder was used. First push the start button. The test takes 15 minutes to complete, and the duty cycles are 18.6, 13.8 and 7.4%, respectively. We choose the pieces at random to determine the order of execution of 9 tests using a table with the encoded values and the number of pieces recorded. The coded values represent parameter changes within a specified range of 3 minimum, average and maximum surfaces. Also, Table 3 for conducting experiments is considered in accordance with the Taguchi experimental design with three surfaces of regulation for each input variable, with the parameters settings and the number of tests required by the Minitab software.

After performing each test and finishing the coating operation, we first cleaned the workpiece with a solution of acetone; then, we re-weighed and weighted the amount of MRR

Table 2 Regulatory parameters and their values in experiments.

Real values	Encoded values		
	Minimum surface (1) − 1 (Low)	Medium surface (2) 0 (Medium)	Maximum surface (3) + 1 (High)
A: Current intensity I(A)	6	12	21
B: Pulse Clear Time $T_{on}(\mu s)$	35	50	100
C: Concentration of β-TCP powder (g/lit)	0	4	8

Table 3 Designed experiments in accordance with the Taguchi test design for three input parameters in three surfaces of regulation.

C1	C2			C3	C4	C5
Run	A	B	C	A, I	B, t_{on}	C (Powder concentration)
1	1	1	1	6	35	0
2	1	2	2	6	50	4
3	1	3	3	6	100	8
4	2	1	2	12	35	4
5	2	2	3	12	50	8
6	2	3	1	12	100	0
7	3	1	3	21	35	8
8	3	2	1	21	50	0
9	3	3	2	21	100	4

Table 4 Encoded values of the input parameters along with the MRR values for each experiment.

C1	C2			C3	C4	C5
Run	A	B	C	Miw	Mfw	MRR
1	− 1	-1	-1	6.965	6.822	2.11
2	− 1	0	0	7.102	6.875	3.363
3	− 1	1	1	6.841	6.790	0.756
4	0	− 1	0	7.024	6.833	2.83
5	0	0	1	6.994	6.687	3.511
6	0	1	− 1	6.763	6.657	1.57
7	1	− 1	1	7.117	6.915	2.993
8	1	0	− 1	7.035	6.753	4.178
9	1	1	0	6.905	6.768	2.03

for each individual piece. These values, as well as the regulatory requirements of each test, are presented in Table 4.

In order to study the surface morphology of the parts, including surface microcracks, surface cavities, porosity and β-tricalcium phosphate particles determination, a scanning electron microscope model (FE-SEM, GEOL 7600F) was used. Surface element distribution has been improved through the use of EDS sensors. The thickness of the deposited layer was examined using cross-sectional morphology. Cross sections of the specimens were prepared by assembly and polishing. To determine the phase composition, an x-ray analysis with CuKα radiation at 45 KV, 40 m_A was used at an angle of 2θ. The improvement of surface micropropagation of powdered β-tricalcium phosphate was investigated by the microarray hardness model (HMV-G21ST). The microhardness is mea-

sured at 0.2 N times in a 15-second period. To reduce the error, each test was repeated on two occasions.

3. Results and Discussion

3.1 Effect of AM-EDM Process Parameters on Material Removal Rate (MRR)

3.1.1 Statistical Tests. The variance analysis results showed that the contribution of input parameters such as discharge current, pulse time and powder concentration was 20, 30 and 40%, respectively. MRR is most affected by the powder concentration. Figure 2 depicts the signal-to-noise ratio for the incidence rate or effect of input parameters on the MRR. As shown, it increases with an increase in the discharge current of the MRR. The optimum mode takes place at the highest rate (3, 2, 3). This includes a 21A current, a pulse duration of 50 μs and a powder concentration of 8 g/lit.

3.1.2 Effect of Pulse Duration on MRR. Figure 3 shows the effect of pulse duration on the removal rate of Ti-6Al-4V alloy materials under powdery and powdery conditions (8 gr/lit). In either case, it is shown that with an increase in pulse time, the amount of MRR increases in the period from 35 to 50 μs. But after that, the MRR is gradually goes down. The reason for this is that in pulse times less than 100 microseconds (<100 μs), the pulse width increases, and in other words, it can be said that the time needed to transfer the discharge energy to the place. It is well thought out that this creates uniform spark frequencies work at the surface of the piece and the incisions are carried out uniformly. In ratios of more than 100 microseconds (>100 μs), the energy density of the discharge
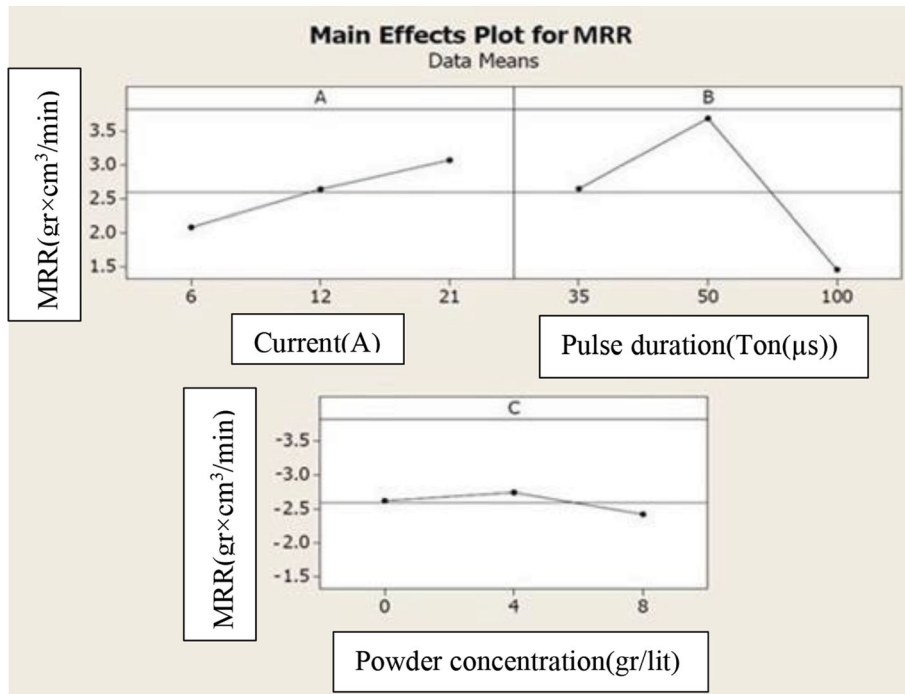
Fig. 2 Chart of the main effects of input parameters on MRR
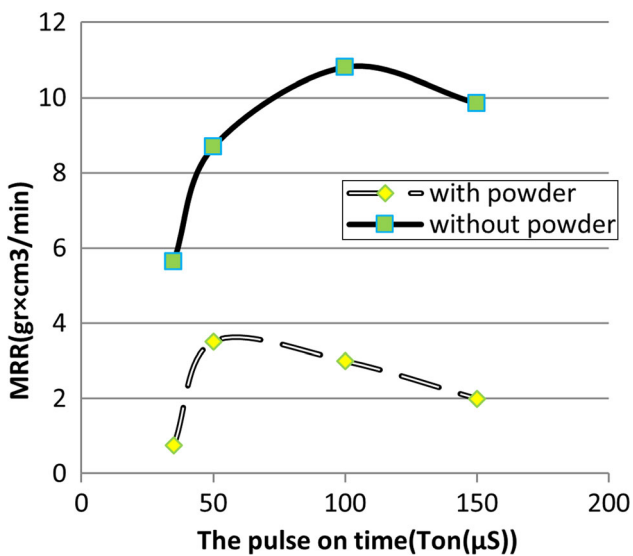

Fig. 3 Effect of pulse duration time on MRR in powdered and non-powdered mode

decreases due to the expansion of the plasma channel, which means that MRR is not done well. Although the extended channel can still melt part of the surface of the workpiece, it cannot produce the right explosive pressure to remove the spray. In addition, the temperature of the workpiece decreases because of the heat transfer from the surface of the workpiece and the expansion of the plasma channel.

In non-powder mode, the amount of spark energy increases as the pulse time increases. In fact, when the pulse's clear time increases, the machine operation time and the number of sparks between the tool and the workpiece will increase, which will increase the loading rate, and this increase will be reduced until the plasma channel is not stable. In conjunction with the

powder, initially, by adding particles to the dielectric circuit, the electrical discharge boost increases which causes better cleaning of locks in the area between tools and sparks do better with stored energy. By increasing the pulse duration, the plasma channel is expanded and the sparks need to store more energy to evacuate it to be cut, but due to the presence of particles in the dielectric, there is a process malfunction which results in less harvesting at the workpiece surface.

3.1.3 Influence of the Intensity of the Current on the MRR. Figure 4 shows the diagram of the variations in the rate of jet propagation from the surface of the Ti-6Al-4V alloy in terms of the two parameters of the discharge current (A) and the pulse duration (B). In this case, the third parameter, the powder concentration, is not efficient and is considered to be 4 grams per liter ($C = 4$ gr/lit). As indicated on the figure, with an increasing discharge current, the MRR value is high. However, as the present rate increases, the energy of sparks also increases. As the current increases, more electric energy is converted into thermal energy, and therefore, more energy is applied to the workpiece, tool and dielectric fluid. This energy is high through the plasma channel to the surface of the workpiece and is transmitted, which exacerbates the melting of the workpiece and evaporates the dielectric material, and as a result, the amount of material will be removed from the workpiece and the MRR will increase.

3.1.4 Impact of Powder Concentration on MRR. Figure 5 shows the development of the powder density in the dielectric on the material removal rate of the Ti-6Al-4V alloy surface. This shows that there is an optimal value for the lowest material removal rate and that the removal rate is increasing. The influence of the addition of phosphate calcium powder on the removal rate of the material is studied by the extent of the gap and the voltage current variations. According to Schumacher, by adding the powder to the dielectric discharge
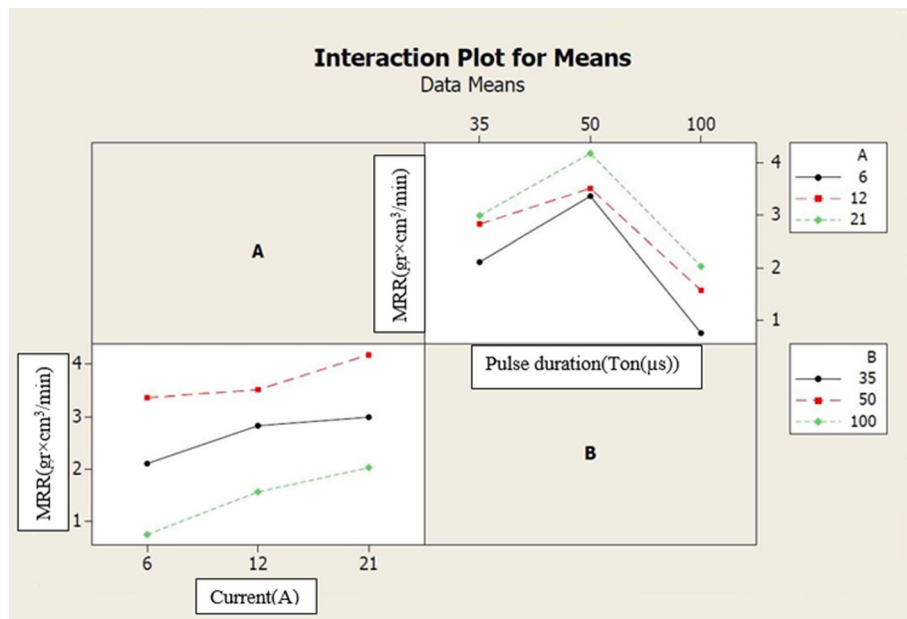
Fig. 4 Interaction diagram of the effect of two current parameters (A) and a pulse (Ton) duration on the MRR
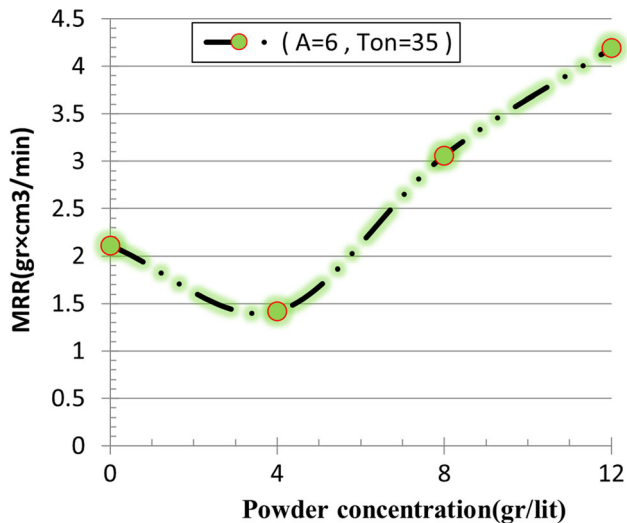

Fig. 5 Effect of powder concentration on MRR in constant current and pulse on time

process, a phenomenon known as bypass will occur (Ref 37). This phenomenon presents different degrees, which can enhance the process if its value is low. The presence of powder particles in the dielectric leads to a reduction in the specific gap resistance and the apparatus increases the gap between two electrodes in order to adjust the resistance. Using electrical conductive particles such as silicon, graphite, titanium and aluminum increases gap distance, these powder particles cause the ions to be transferred better and create a uniform electrical discharge energy, which eventually increases the material removal rate. However, given that calcium phosphate powder does not have conductivity properties, the distance between the two will be reduced and the electrical discharge will not be uniform. As a result, the system produces a small electrical discharge space for dielectric failure which causes a reduction

in the material disposal rate. When the powder density increases, there is a significant decrease in the gap distance, and due to the high accumulation of particles on the alloy surface, due to electrical discharge the system must save more spark energy. In this case, the spark will be created with higher blast power on the surface, and hence, the rate of material removal is increased.

3.2 Effect of AM-EDM Process Parameters on Surface Roughness (SR)

3.2.1 Effect of Spark Energy on Surface Roughness. Figure 6 shows the main effect of the spark energy on surface roughness (SR) in powder and non-powdered state in the process of electrical discharge.

As the chart shows, the surface roughness increases overall as a function of energy. The reason for this is the increase in the energy of the electric discharge transferred to the tool and the workpiece and the separation of the larger cuttings, thereby creating deeper holes and depressions and increasing surface roughness. When the peak current rises from 6 to 12 A, the surface roughness rises from 6.4 to 8.6 to 2.2 μm. This condition happens when no powder is present. When we use a concentration of 4 g/lit in a process, the surface roughness increases from 5.1 to 5.3 per 0.2 μm. In conjunction with powder, due to the dispersion of particles in deionized water, the uniformity of the ignition areas is reduced and the electrical evacuation chip increases to some extent from the non-powdery state, resulting in the generation of thermal energy from electric sparks in Dielectric solution. As a result, small sizes and pitting are developed on the machining surface and the amount of surface roughness decreases with respect to the non-wet state.

3.2.2 Impact of pulse duration on surface roughness

Figure 7 shows the main effect diagram of the Ton period on the surface roughness (SR) in powderless and powdered state in the process of electrical discharge.

As illustrated in the graph, the surface roughness increases as a function of energy. This is due to the increased discharge capacity as well as the increased power of electric sparks and
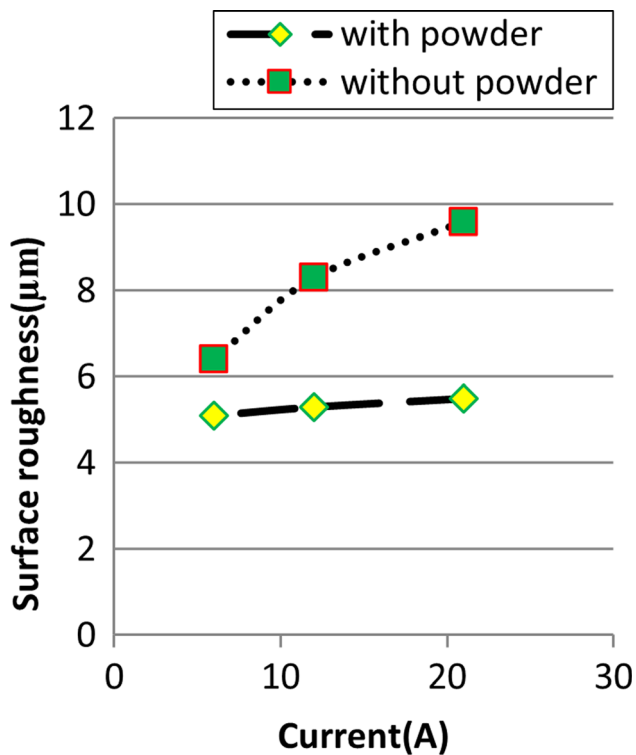
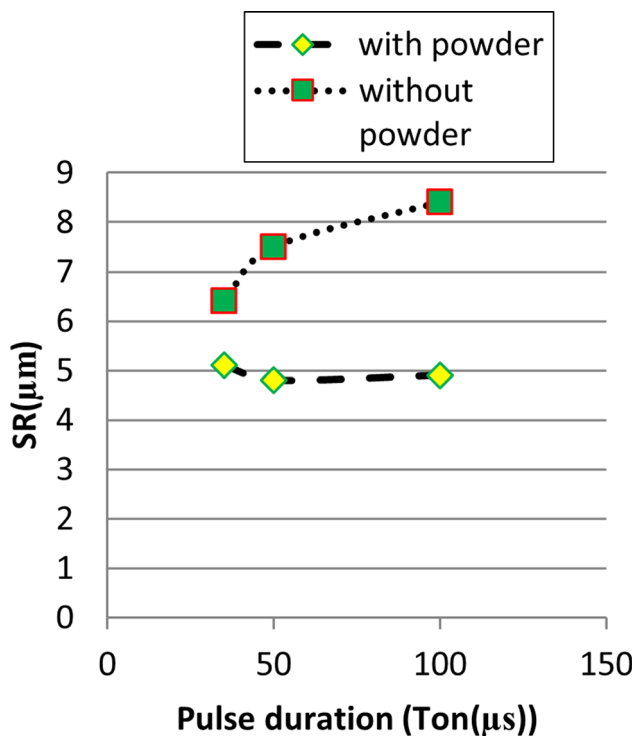**Fig. 6** Main effect of the current intensity (A) on surface roughness (SR)

Fig. 7 Main effect diagram of the pulse duration (Ton) on surface roughness (SR)

the deep penetration in the workpiece. As a consequence, the size of the cavities generated by the sparks increases, making the surface of the part more rigorous and increasing the roughness parameter (Ra). When the pulse time is 35 to 100 μs,

the surface roughness changes from 6.4 to 8.4 to 2 μm. This condition happens when no powder is present. When using a 4 g/lit concentration during the process, the surface roughness decreased from 5.1 to 4.8 per 0.3 μm. In the case of powder, because of the dispersion of particles in deionized water, the distance between the two electrodes is increased and the washings are better. It also increases the heterogeneity of frequencies and sparks, which reduces the expanses and pits at the surface. With pulse duration between 50 μs and 100 μs, surface roughness also increases. The reason for this is the reduction in the electrical discharge, the increase in the plasma channel and the accumulation of particles on the surface of the workpiece, in which the sparks require a large amount of energy to get rid of the surface, which also causes sudden discharge with severity of degradation heating up, and a lot of heat moves to the surface. Due to the fact that there is no good rinsing in the process, the surface heat transfer is reduced, which reduces the resistance to erosion sparks.

3.2.3 Impact of powder concentration on SR

Figure 8 shows the main effects graph of input parameters on surface roughness (SR) in powder and non-powdered state in the process of electrical drainage if two other input parameters in each graph are assumed to be constant according to Table 2.

As the graph shows, the roughness of the surface is reduced by first adding the powder. The reason is that the effect of the collision of electric sparks on the surface and sparks are not evenly distributed among powder particles. As a result, less electrical discharge occurs, and loading from the workpiece surface is irregularly done so that the device creates a gap between the two electrodes to compensate for this. As a result, a better thaw is carried out and, lastly, holes with a shallow depth are created. This will make it possible to improve the surface quality. However, when the powder concentration increases, the heat energy of the workpiece surface increases as the solution warms. This is due to the reduction in machining chains and the high energy consumption on the surface of the cutting part. The appliance starts to oscillate and produces an uneven discharge with a high intensity effect. As a result of this, mold pans are formed wider and deeper at the workpiece surface, which ultimately leads to the quality of the lower surface of the workpiece.

3.3 Examination of Surface Properties Improved by the Process of Discharging with an Additive Mixed EDM (AM-EDM)

3.3.1 Morphology of the Modified Surface. Figure 9 shows the surface morphology enhanced by the removal process in deionized water in the presence of powder-free β-TCP. In this shape, the volcanic craters created by the electrical discharge of the sparks are visible on both surfaces. Figure 9(a) and (b) shows the EDM surface in non-powdered condition. As shown in the figure, fused materials, surface cracks and cavities are observed. With a magnification of 1500 times the surface of the EDM, the quality of the lower surface is visible. The reason for this is the increase in the thermal energy at the surface of the workpiece, which causes the depleted materials to be deposited on the surface and the formation of deep and wide openings in the sedimentary boundaries. Figure 9(c) and (d) shows the surface of AM-EDM processed with β-tricalcium phosphate powder at a concentration of 4 g/lit in deionized water. On the
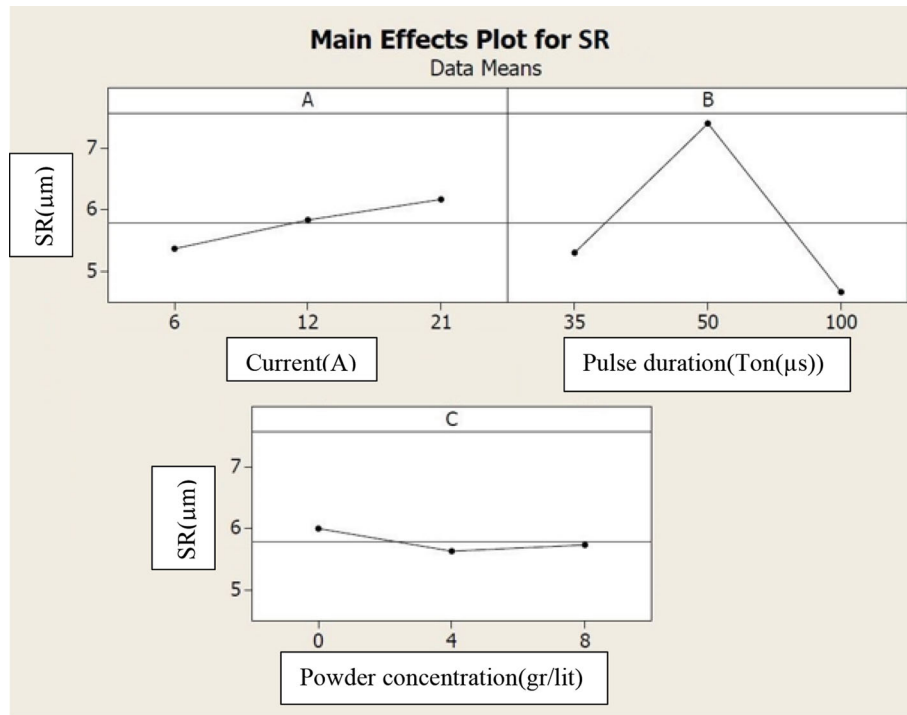
Fig. 8 Main plot of the impact of the powder concentration (gr/lit) on surface roughness (SR) and effects of current , pulse duration and powder concentration on surface roughness
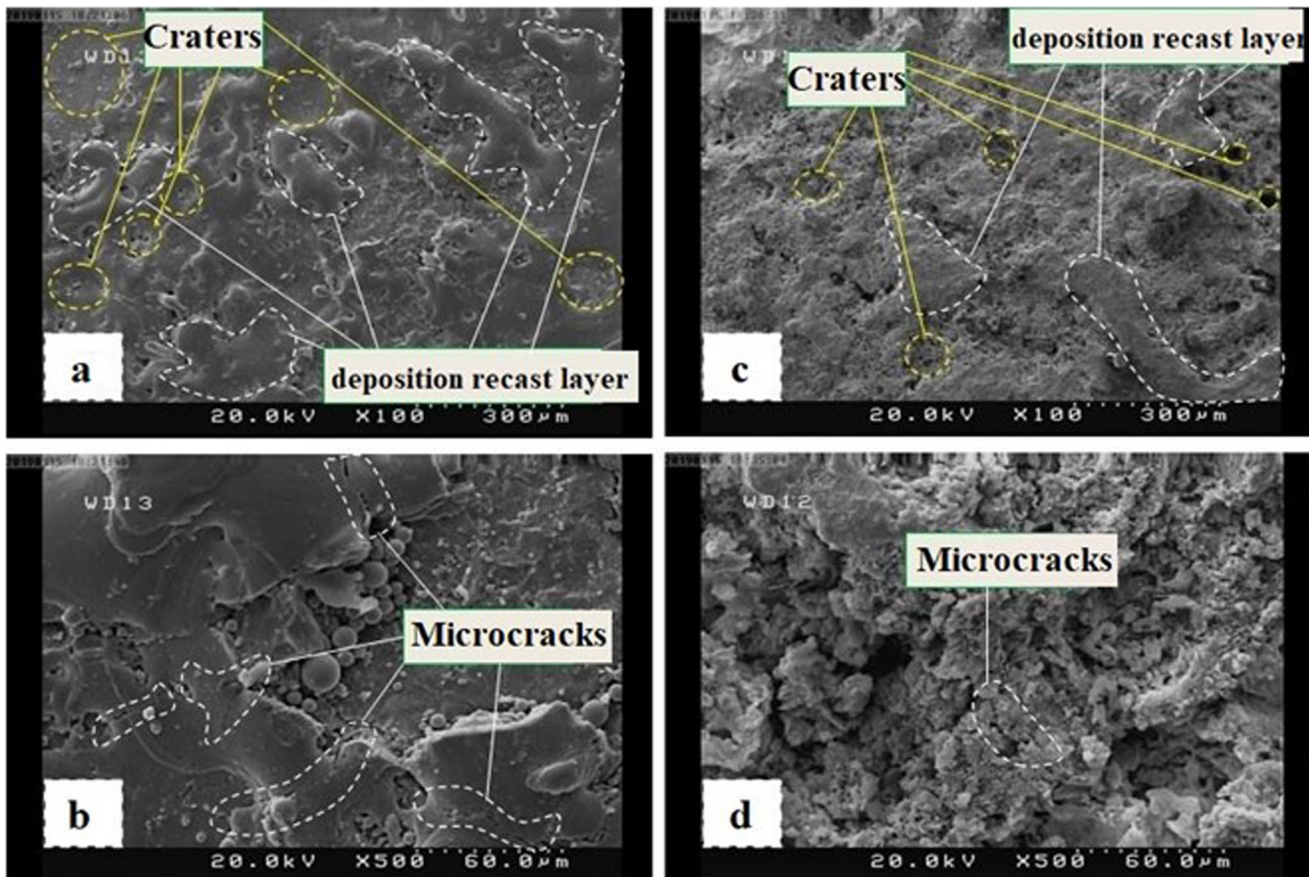

Fig. 9 Surface morphology of the Ti-6Al-4V alloy in the powderless EDM process: (a) magnification 250 times, (b) magnification of 1500 times, and in the AM-EDM process with β-TCP powder (c) magnification of 250 times and (d) magnification of 1500 times under 6A and a pulse duration of 35 μs

AM-EDM-enhanced surface, the number and diameter of cavity openings are less than the EDM surface. The reason for this is the short circuit and also the creation of abnormal (non-uniform) frequencies in a dielectric containing β-tricalcium phosphate powder, which, as a result, reduces the number of electrical discharge and increases the surface quality. Moreover, a small amount of microcracks and dust particles deposited is clearly visible. Due to the presence of particles in dielectrics and failure of water transfusion due to chemical reactions during the process of AM-EDM, it forms at the surface of the oxide and carbide sample. By adding the powder to the EDM process, we can see a spectacular reduction in surface cracks.

3.3.2 Impact of the Concentration on the Morphology of the Surface.

Figure 10 shows the morphology of the surface enhanced with AM-EDM at concentrations of 8 g/l and 12 g/l under similar working conditions according to Table 3.2. Figure 10(a) shows the precipitation of β-TCP powder at a concentration of 8 g/l and without striation. In Fig. 10(b), with the exception of particles created at the surface of β-TCP deposition, a significant amount of oxide in high ratios is clearly seen on surface layers at a magnification of 5000 times. It is common knowledge that porosity plays an important role in cell activity and improves the functioning of implants. In Fig. 10(c), when the concentration of β-TCP powder increases (12 g/l), a denser, more even layer of oxide and hydride will precipitate onto a layer of β-TCP. In Fig. 10(d), due to the increase in the concentration of β-tricalcium phosphate powder, nanoporosity is observed with a lower density at an improved surface at a magnification of 12000 times. During the AM-EDM process, due to the production of water vapor and hydrogen gas, β-TCP boundaries and superficial nanoporosity are generated which can increase surface energy and wettability and improve cell adhesion performance. During the coating process, due to the thermal energy generated, a large amount of water vapor is generated, which leads to a chemical reaction between the metals and β-TCP powder elements, which can produce hydrogen gas.

3.3.3 The Thickness of the Modified Layer.

Figure 11 shows a thin layer of β-TCP powder at various strengths (4 g/l, 8 g/l and 12 g/l). Figure 11(a) measures the thickness of the deposited layer at a concentration of 4 g per liter at approximately 3.73 microns. This is a thin layer not uniform with abundant deposition. The deposited layer depends on the spark discharge energy and the evaporation space (chip) is increased due to the presence of powder particles in the deionized water. As a result, because of the reduced energy of spark discharge, less material is removed evenly from the surface of the workpiece. As a result, by increasing the discharge chute, proper washing occurs at the debris formation site, which reduces the deposition of material on the machining surface. In Fig. 11(b) and (c), the thickness of the deposited layer increases with increasing concentrations of β-tricalcium phosphate powder. The thickness of the deposited layer at concentrations of 8 g/l and 12 g/l is measured at around 15.33 and 35 μm, respectively. The thickness of the deposited layer depends on the phenomenon of transportation of the material by electrostatic forces. Increasing the concentration of β-TCP powder in
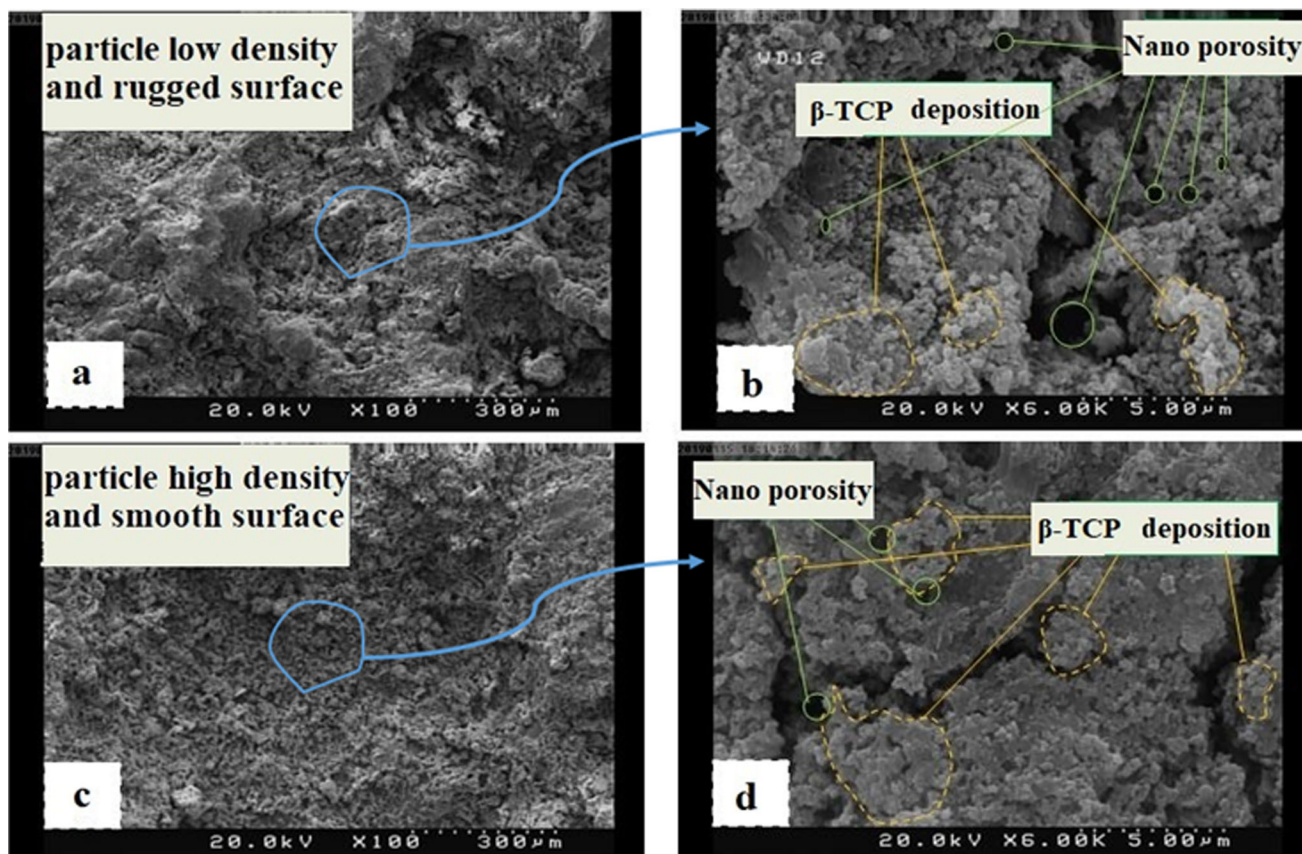

Fig. 10 SEM micrographs of the surface enhanced by AM-EDM in the display of β-TCP and nanoporosity in a concentration of 8 g/L: (a) magnification of 250 times, (b) magnification of 12,000 times and 12 g/L, (c) magnification of 250 times and (d) magnification of 12,000 times
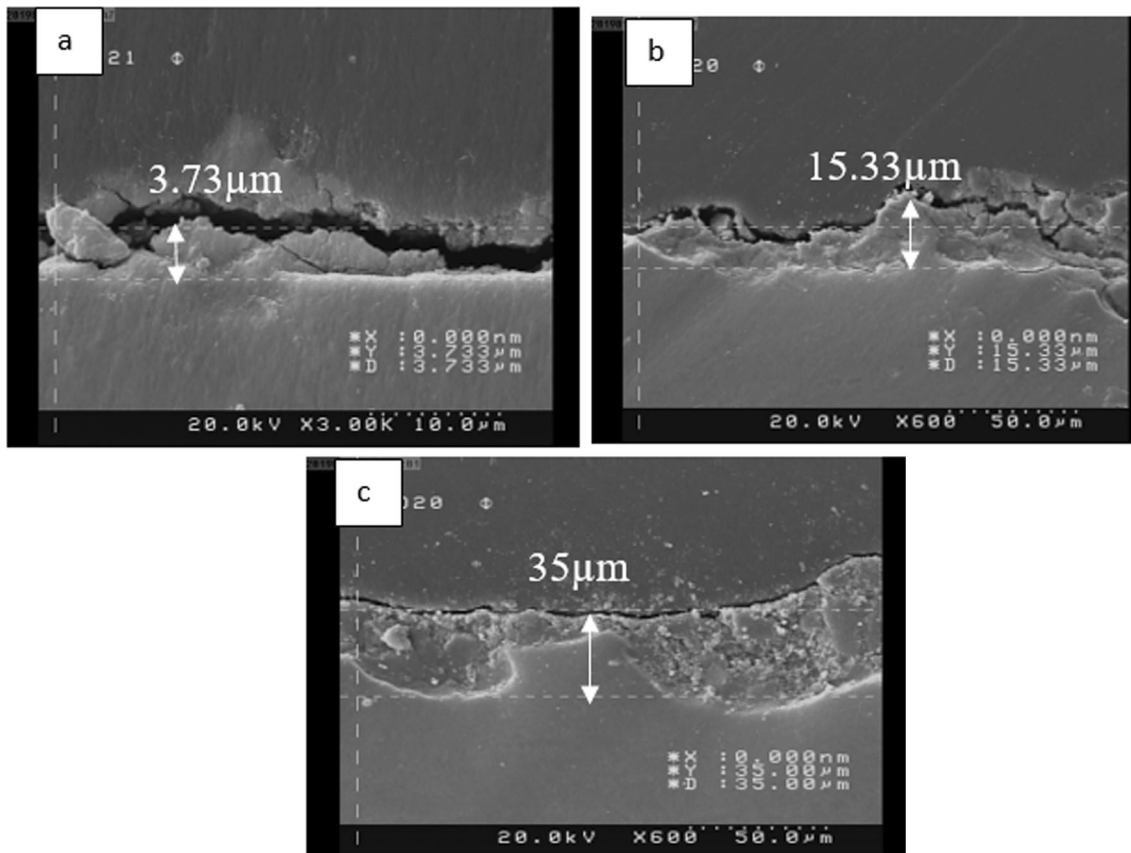
Fig. 11 Micrographic transverse section of the layer deposited in the AM-EDM process at different concentrations of β-TCP powder ((a) 4 grams per liter, (b) 8 grams per liter, (c) 12 grams per liter) under operating conditions, intensity of 6 amps and clear time pulse 35 microseconds

the distance between the small chip and the absorbed particles of the powder together with the depleted remains of the electrodes, which is displaced by the phenomenon of transfer of materials and electrostatic forces toward the workpiece, which ultimately causes precipitation and increase in the thickness reset.

3.3.4 Morphology of Improved Surface (Elemental) Compounds. Figure 12 clearly illustrates the AM-EDM enhanced interface line and the EDM surface. In Fig. 12(a), on the surface of the EDM, the microstructure of the surface shows defects such as cracks and the lack of β-tricalcium phosphate particles. The presence of surface defects decreases the adhesion resistance of the connection line. As a result, the EDM surface creates a low bond between the substrate and the coating, resulting in long-term corrosion and fracture fatigue. As shown in Fig. 12(b), on the surface of the AM-EDM, the undersurface coating is clearly visible, indicating a strong adhesion between the substrate and the coating. The relationship between the underlying line and the coating line depends upon the beginning of the chemical binding in the process. In case of surface porosity, bone marrow adhesion and bone tissue integrity are helpful to create a strong bond between substrate and porous coating.

Figure 13 depicts the sample models, the EDM performed and the EDM-AM performed on the EDS spectrometers. In Fig. 13(a), the EDS spectrometer shows the surface of the EDM surface of the Ti, Al and V elements on the surface, which is one of the basic elements of Titanium Grade 5 alloy. In

addition, the O2 element is also visible at the surface. Oxygen appears to produce oxides during the EDM process. This is due to the evaporation of high water temperatures due to the generation of thermal energy in the plasma canal. In Fig. 13(b), from the EDS surface diagram in the AM-EDM process, along with β-tricalcium phosphate powder, the elements O, Ca, P and also a part of Ti, Al and V elements are seen. The presence of O, Ca and P elements at the sample surface improved by the AM-EDM process is due to the decomposition of β-tricalcium phosphate powder in the deionized water. As a result of the chemical reaction of the elements O, Ca and P in the molten pool formed on the surface of the workpiece, oxides and hydrides are formed. Reports have shown that the formation of O, Ca and P components should produce a good chemistry surface for bone formation and implantation.

In Fig. 14(a) in the model obtained from the EDM surface XRD spectrometer, the Ti-α and Ti-β phase. Apparently, the EDM process causes changes in surface chemistry as a result of the chemical reaction of the fusion elements with the dielectric fluid. In Fig. 14(b), the XRD scheme is modeled on the surface of the AM-EDM and shows the formation of biocompatible phases on the enhanced surface. The oxide and hydride phases predicted on the surface of the AM-EDM are $Ca_2P_2O_7$ and $Ca(OH)_2$, respectively. Variations in the TCP composition can lead to various precipitation phases such as calcium pyrophosphate $(Ca_2P_2O_7)$ and calcium hydroxide $(Ca(OH)_2)$ as both are interesting for bone replacement. The Constitutional the chemical reaction of β-TCP powder, surfac-
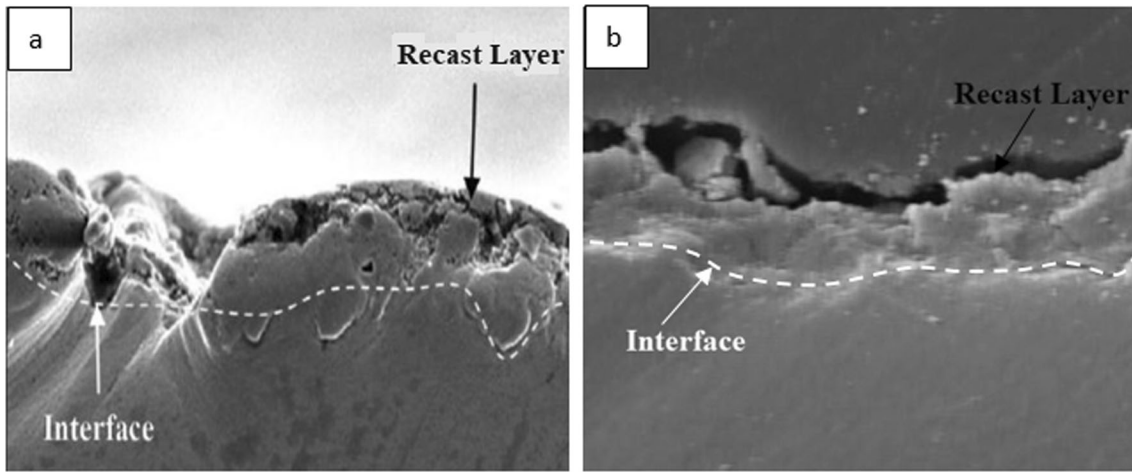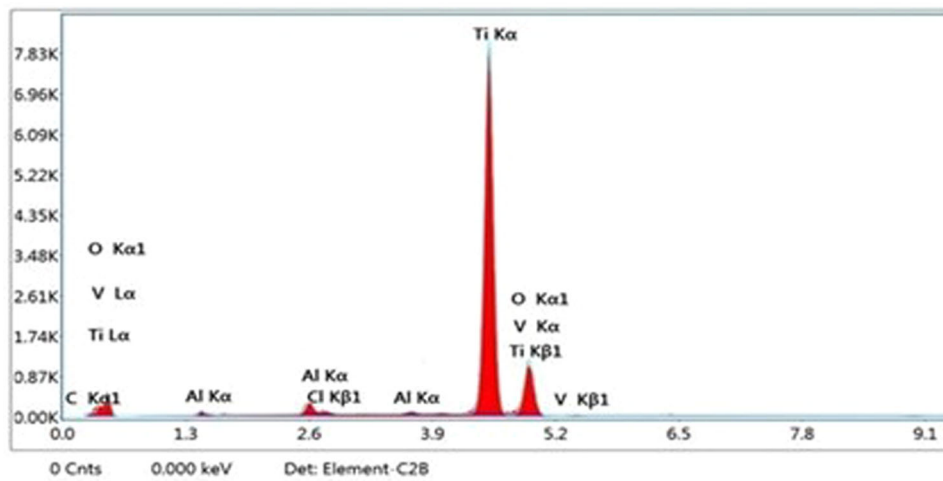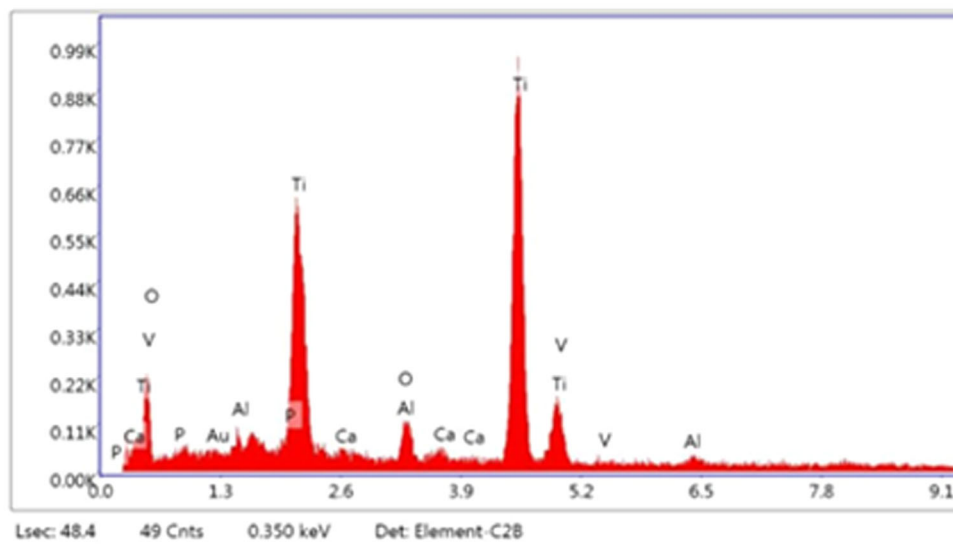
Fig. 12 SEM micrograph of improved layer adhesion: a) in the absence of β-TCP powder, b) in combination with β-TCP powder

Fig.13 (a) Element distribution diagram is done in the process of EDM. (b) Distribution diagram of elements in the process of AM-EDM with β-TCP powder
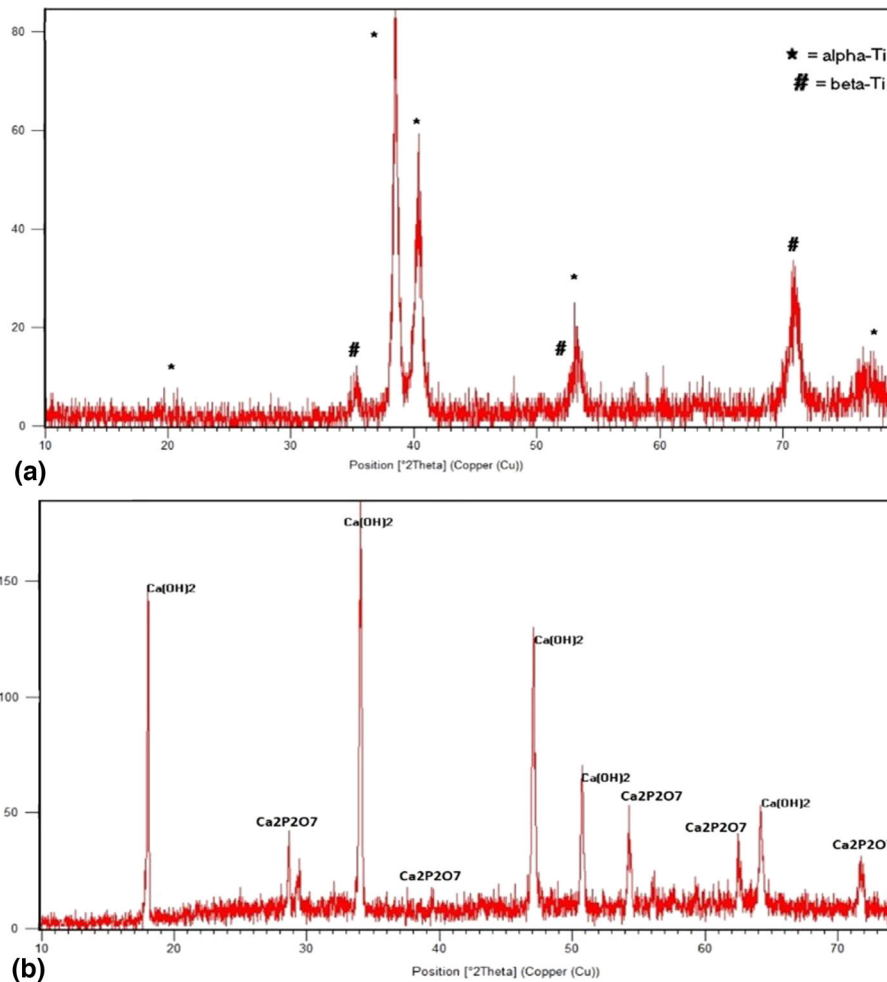
Fig. 14 (a) XRD pattern of Ti-6Al-4V alloy surface in EDM process . (b) XRD pattern of Ti-6Al-4V alloy surface in AM-EDM process with β-TCP powder

tant, oxygen and hydrogen produced from water vapor and the main elements of the alloy. As a result, those phases stimulate the bioavailability of the alloy to the bone formation (strong bond) between the alloy and the natural bone tissue.

3.3.5 Improved Surface Microhardness. In Fig. 15, the microlayer AM-EDM sample is made of β-TCP on the surface of the Ti-6Al-4V alloy. By measuring the undeveloped surface microhardness (EDM), the amount of 240HV is achieved. While the microenvironment enhanced with β-TCP (AM-EDM Made), 348 HV were featured, which is approximately 2.5 times more than the non-machine alloy. After the EDM process, the surface hardness of the workpiece is 1.75 times, since the hard oxide phase is formed on the seam. Likewise, after the surface has been improved by the AM-EDM process, the surface hardness of the workpiece is 2.5 times. This may be due to the formation of the solid phase $Ca_2P_2O_7$ and $Ca(OH)_2$ on the upgraded surface of the grade 5 alloy titanium layer. This coating can increase the resistance to corrosion and abrasion many times the alloy used in medical implants. Moreover, due to the biomimetic hydrides and oxide formed on the alloy surface, it can increase the fatigue resistance and improves the
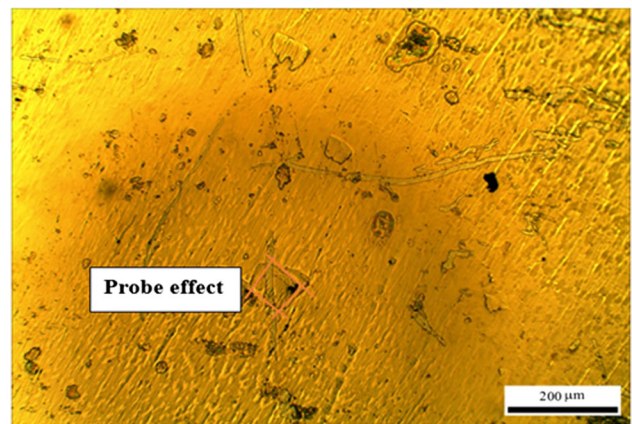

Fig. 15 Effect of Vickers' microhardness probe on the surface modified by AM-EDM

compatibility of the alloy for long-term use. In Fig. 15, the effect of the microtreatment vice is observed in the re-gluing line and the subsurface layer.

4. Conclusion

In this study, AM-EDM was used to cover surfaces of Ti-6Al-4V alloy, which was successfully applied to the coating powder for the β-tricalcium phosphate coating. Results from this study have shown:

- Formation of a β-TCP layer, the porosity of which is relatively uniform with the quantity of 10 to 21 micrometers deposited. To continue deposition, β-tricalcium phosphate coatings can be better obtained by increasing the concentration of particulate matter in deionized water.
- At a concentration of 12 g/L of powder, a very thick and dense layer of β-TCP with a size of 35 μm was deposited on a Ti alloy surface. The chemical reaction of the Ti-6Al-4V alloy elements, water vapor, glycerin, β-TCP and calcium chloride consisted of Ca, P, O, Ti, H and Al.
- The XRD diagram shows the development of biomimetic phases, such as $(Ca_2P_2O_7 . Ca(OH)_2)$ in coated nanoporous layers.
- With increasing current and pulse duration, the amount of surface roughness (SR) increases, but this amount is low in the process of improving the surface along with the powder compared to the process without powder, with the lowest SR measured to be 4.3 micrometer.
- The β-TCP coating increases the microhardness of the grade 5 titanium substrate by 348 HV, 1.75 times that of the untreated surface.
- The layer containing β-TCP, the properties of corrosion resistance and biomimetic oxidation improve the biological properties of the surface and reduce the degradation of the alloy surface against the immune system or prevent the release of toxic elements in the body, and the failure of the treatment prevents re-implant-related surgeries.

Funding

References

1. C. Fleck and D. Eifler, Corrosion, Fatigue and Corrosion Fatigue Behaviour of Metal Implant Materials, Especially Titanium Alloys, *Int. J. Fatigue*, 2010, **32**(6), p 929–935
2. H. Ghonem, Microstructure and Fatigue Crack Growth Mechanisms in High Temperature Titanium Alloys, *Int. J. Fatigue*, 2010, **32**(9), p 1448–1460
3. K.S. Chan, Changes in Fatigue Life Mechanism Due to Soft Grains and Hard Particles, *Int. J. Fatigue*, 2010, **32**(3), p 526–534
4. C.J. Boehlert et al., Fatigue and Wear Evaluation of Ti-Al-Nb Alloys for Biomedical Applications, *Mater. Sci. Eng., C*, 2008, **28**(3), p 323–330
5. J.J. Williams and N. Chawla, Fractography of a Neck Failure in a Double-Modular Hip Implant, *Case Studies in Engineering Failure Analysis*, 2014, **2**(1), p 45–50
6. S. Kumar, R. Singh, T.P. Singh, and B.L. Sethi, Surface Modification by Electrical Discharge Machining: A Review, *J. Mater. Proc. Technol.*, 2009, **209**(8), p 3675–3687
7. T. Muthuramalingam and B. Mohan, A Review on Influence of Electrical Process Parameters in EDM Process, *Arch. Civil Mech. Eng.*, 2015, **15**(1), p 87–94
8. R.A. Gittens et al., The Effects of Combined Micron-/Submicron-Scale Surface Roughness and Nanoscale Features on Cell Proliferation and Differentiation, *Biomaterials*, 2011, **32**(13), p 3395–3403
9. K. Kieswetter et al., The Role of Implant Surface Characteristics in the Healing of Bone, *Crit. Rev. Oral Biol. Med.*, 1996, **7**(4), p 329–345
10. Z. Schwartz and B.D. Boyan, Underlying Mechanisms at the Bone-Biomaterial Interface, *J. Cell. Biochem.*, 1994, **56**(3), p 340–347
11. J.Y. Martin et al., Effect of Titanium Surface Roughness on Proliferation, Differentiation, and Protein Synthesis of Human Osteoblast-Like Cells (MG63), *J. Biomed. Mater. Res.*, 1995, **29**(3), p 389–401
12. B.D. Boyan et al., Osteoblast-Mediated Mineral Deposition in Culture is Dependent on Surface Microtopography, *Calcif. Tissue Int.*, 2002, **71**(6), p 519–529
13. Y.T. Sul et al., Optimum Surface Properties of Oxidized Implants for Reinforcement of Osseointeg Ration: Surface Chemistry, Oxide Thickness, Porosity, Roughness, and Crystal Structure, *Int. J. Oral Maxillofac. Implants*, 2005, **20**, p 3
14. X. Liu, J.Y. Lim, H.J. Donahue, R. Dhurjati, A.M. Mastro, and E.A. Vogler, Influence of Substratum Surface Chemistry/Energy and Topography on the Human Fetal Osteoblastic Cell Line hFOB 1.19: Phenotypic and Genotypic Responses Observed in Vitro, *Biomaterials*, 2007, **28**(31), p 4535–4550
15. F. Rupp et al., Enhancing Surface Free Energy And Hydrophilicity Through Chemical Modification of Microstructured Titanium Implant Surfaces, *J. Biomed. Mater. Res. Part A Off. J. Soc. Biomater. Jpn Soc Biomater Aust. Soc. Biomater. Korean Soc. Biomater.*, 2006, **76**(2), p 323–334
16. G. Zhao et al., High Surface Energy Enhances Cell Response to Titanium Substrate Microstructure, *J. Biomed. Mater. Res. Part A Off. J. Soc. Biomater. Jpn. Soc. Biomater. Aust. Soc. Biomater. Korean Soc. Biomater.*, 2005, **74**(1), p 49–58
17. Z. Schwartz, P. Raz, G. Zhao, Y. Barak, M. Tauber, H. Yao, and B.D. Boyan, Effect of Micrometer-Scale Roughness of the Surface of Ti-6Al-4V Pedicle Screws in vitro and in vivo, *J. Bone Joint Surg. Am. Vol.*, 2008, **90**(11), p 2485
18. W Att et al. Effect of Supramicron Roughness Characteristics Produced by 1-and 2-Step Acid Etching on the Osseointegration Capability of Titanium. Int. J. Oral Maxillofac Impl 22 5 (2007)
19. S.L. Chen et al., Effect of Electro-Discharging on Formation of Biocompatible Layer on Implant Surface, *J. Alloys Compnd.*, 2008, **456**(1–2), p 413–418
20. AA Aliyu et al. A Review of Additive Mixed-Electric Discharge Machining: Current Status and Future Perspectives for Surface Modification of Biomedical Implants. Adv. Mater. Sci. Eng. (2017)
21. T. Chang-bin, L. Dao-Xin, W. Zhan, and G. Yang, Electro-Spark Alloying Using Graphite Electrode on Titanium Alloy Surface for Biomedical Applications, *Appl. Surf. Sci.*, 2011, **257**(15), p 6364–6371
22. P. Harcuba, L. Bačáková, J. Stráský, M. Bačáková, K. Novotna, and M. Janeček, Surface Treatment by Electric Discharge Machining of Ti-6Al-4V Alloy for Potential Application In Orthopaedics, *J. Mech. Behav. Biomed. Mater.*, 2012, **7**, p 96–105
23. H.M. Chow, L.D. Yang, C.T. Lin, and Y.F. Chen, The use of SiC Powder in Water As Dielectric for Micro-Slit EDM Machining, *J. Mater. Proc. Technol.*, 2008, **195**(1–3), p 160–170
24. Z.J. Xie et al., Titanium Carbide Coating with Enhanced Tribological Properties Obtained by EDC Using Partially Sintered Titanium Electrodes and Graphite Powder Mixed Dielectric, *Surf. Coat. Technol.*, 2016, **300**, p 50–57
25. C. Prakash, H.K. Kansal, B.S. Pabla, and S. Puri, Experimental Investigations in Powder Mixed Electric Discharge Machining of Ti-35Nb-7Ta-5Zrβ-titanium alloy, *Mater. Manuf. Proc.*, 2017, **32**(3), p 274–285
26. S.K. Sahu, T. Jadam, S. Datta, and G. Nandi, Effect of Using SiC Powder-Added Dielectric Media During Electro-Discharge Machining of Inconel 718 Superalloys, *J. Braz. Soc. Mech. Sci. Eng.*, 2018, **40**, p 1–9
27. M.B. Ndaliman, A.A. Khan, and M.Y. Ali, Influence of Dielectric Fluids on Surface Properties of Electrical Discharge Machined Titanium Alloy, *Proc. Inst. Mech. Eng. Part B J. Eng. Manuf.*, 2013, **227**(9), p 1310–1316

28. M. Umar Farooq, M. Pervez Mughal, N. Ahmed, N. Ahmad Mufti, A.M. Al-Ahmari, and Y. He, On the Investigation of Surface Integrity of Ti-6Al-4V ELI Using Si-Mixed Electric Discharge Machining, *Materials.*, 2020, **13**(7), p 1549

29. T.T. Öpöz, H. Yaşar, N. Ekmekci, and B. Ekmekci, Particle Migration and Surface Modification on Ti-6Al-4V in SiC Powder Mixed Electrical Discharge Machining, *J. Manuf. Proc.*, 2018, **31**, p 744–758

30. F. Alavi and M.P. Jahan, Optimization of Process Parameters in micro-EDM of Ti-6Al-4V Based on Full Factorial Design, *Int. J. Adv. Manuf. Technol.*, 2017, **92**, p 167–187

31. M.P. Mughal, M.U. Farooq, J. Mumtaz, M. Mia, M. Shareef, M. Javed, M. Jamil, and C.I. Pruncu, Surface Modification for Osseointegration of Ti-6Al-4V ELI Using Powder Mixed Sinking EDM, *J. Mech. Behav. Biomed. Mater.*, 2021, **113**, p 104145

32. A. Schubert, V.D. Bui, I. Schaarschmidt, T. Berger, and A. Martin, Developments in Powder Mixed EDM and its Perspective Application for Targeted Surface Modification, *Procedia CIRP.*, 2022, **113**, p 100–119

33. S.M. Rabiee, F. Moztarzadeh, and M. Solati-Hashjin, Synthesis and Characterization of Hydroxyapatite Cement, *J. Mol. Struct.*, 2010, **969**(1–3), p 172–175

34. M. Bohner, B.L. Santoni, and N. Döbelin, β-Tricalcium Phosphate for Bone Substitution: Synthesis and Properties, *Acta Biomater.*, 2020, **113**, p 23–41

35. V. Singh, R. Bhandari, and V.K. Yadav, An Experimental Investigation on Machining Parameters of AISI D2 steel using WEDM, *Int. J. Adv. Manuf. Technol.*, 2017, **93**(1–4), p 203–214

36. H. Kumar, A. Manna, and R. Kumar, Modeling of Process Parameters for Surface Roughness and Analysis of Machined Surface in WEDM of Al/SiC-MMC, *Trans. Indian Inst. Met.*, 2018, **71**, p 231–244

37. B.M. Schumacher, About the Role of Debris in the Gap During Electrical Discharge Machining, *CIRP Ann.*, 1990, **39**(1), p 197–199